J MATER SCI **41** (2006) 3781–3785

Piezo-spectroscopic characterization of alumina-zirconia layered composites

G. PORTU DE
Institute of Science and Technology for Ceramics, Via Granarolo 64-48018 Faenza, Italy; Research Institute for Nanoscience, RIN, Sakyo-ku, Matsugasaki, 606-8585, Kyoto, Japan

J. GURAUSKIS
Instituto de Ceramica y Vidrio, CSIC, Campus de Cantoblanco, 28049 Madrid, Spain

L. MICELE
Institute of Science and Technology for Ceramics, Via Granarolo 64-48018 Faenza, Italy; Research Institute for Nanoscience, RIN, Sakyo-ku, Matsugasaki, 606-8585, Kyoto, Japan

A. J. SÁNCHEZ-HERENCIA, C. BAUDIN
Instituto de Ceramica y Vidrio, CSIC, Campus de Cantoblanco, 28049 Madrid, Spain

G. PEZZOTTI
Ceramic Physics Laboratory, Kyoto Institute of Technology, KIT, Sakyo-ku, Matsugasaki, 606-8585, Kyoto, Japan; Research Institute for Nanoscience, RIN, Sakyo-ku, Matsugasaki, 606-8585, Kyoto, Japan

Published online: 10 April 2006

Ceramic monolithic and multilayered composites were produced by stacking water based green ceramic cast tapes. Two different mixtures of composites within the Al_2O_3/YTZP, system were investigated. The difference in the coefficient of thermal expansion (CTE) between the composites fabricated, resulted in the development of residual stresses when the same compositions were combined in a multilayered structure. The magnitude and the distribution of these residual stresses were assessed by the piezo-spectroscopic technique. The stress within the layers varied with a parabolic trend, with the highest values at the interfaces and a reduction toward the centre of the layers. The influence of symmetry of the multilayered laminate on the magnitude and distribution of the residual stresses within the structure are discussed.

1. Introduction

Ceramic multilayered composites may undergo residual stresses of remarkable magnitude during sintering and upon cooling from the sintering temperature, especially if they consist of relatively thick layers with a different phase composition. Residual stresses arise from mismatches in sintering rate, coefficient of thermal expansion (CTE) and elastic constant between the constituent phases and among neighbouring layers [1]. Compressive residual stresses are generated, in the layer (or phase) with lower CTE, while tensile residual stresses usually appear in the layer (or phase) with higher CTE. In general, the magnitude of the residual stresses developed in a composite is proportional to the CTE mismatch between the constituents. In a layered structure, the mismatch between the CTE of layers of different composition determines the level of the residual stresses [1]. In order to avoid cracking [2, 3] and delamination [4, 5], a precise control of both magnitude and distribution of residual stresses is mandatory.

As a first approach, residual stresses can be estimated using the CTE and elastic properties of monolithic materials with the same composition of the constituent layers, assuming that no interaction occurs at the interface between layers. In order to evaluate the validity of such an approach and establish a general methodology for the design of laminates, the residual stress profile has to be determined in materials with a tailored stress profile. In order to do so, laminated composites have been prepared by tape-casting in organic solvents [6] and in water based solution [7, 8] and stacking discrete layers having different thickness and composition.

0022-2461
DOI: 10.1007/s10853-006-2508-z

In this work, we present measurements of the residual stress and its dependence on geometry of multilayered ceramics obtained in the system Al_2O_3/YTZP, starting from laminates obtained by water-based cast tapes, using the technique of piezo-spectroscopy applied to the chromophoric fluorescence of Al_2O_3. The piezo-spectroscopic technique was first applied by Grabner in measuring of residual stresses in Al_2O_3 [9] and has been applied to laminated structures as well [10, 11]. In the present paper the stress profile measured through the cross section of the laminated structures was analyzed and related to the layer composition.

2. Theoretical tools: Piezo-spectroscopic measurements

The stress field distribution along the cross section of infiltrated samples was determined by using piezo-spectroscopy techniques related to the characteristic R1, R2 doublet produced by chromophoric fluorescence of Cr^{3+} impurities in Al_2O_3. The principle of relating an observed line shift in a fluorescence spectrum to the state of stress has been described previously by Grabner [9]. When polycrystalline Al_2O_3 (having a fine grained microstructure and no significant texture) is subjected to a stress, the change in frequency Dn in luminescence line is given by the tensorial relationship:

$$\Delta\nu = \frac{1}{3}\,\Pi_{ii}\,\sigma_{jj} \tag{1}$$

where P_{ii} is referred to as the piezo-spectroscopic coefficient (i.e., relating frequency to stress).

The overall residual stress field arises from differences in sintering rate, thermal expansion and elastic mismatch between the constituent ceramic phases of the laminated Al_2O_3/YTZP composite. This stress consists of two separate components: (i) a microscopic stress field originating on the microstructural scale from grain-to-grain thermal and elastic mismatches between Al_2O_3 and YTZP; and, (ii) a macroscopic stress field, so that equilibrium conditions between adjacent layers are established. The approach of measuring only the second contribution of the stress has been previously suggested by the authors [11]; for this reason the frequencies used as a standard value for unstressed material were obtained from monolithic bars fabricated using the same processing route and having the same composition of the constituent tapes as of the laminate.

An important characteristic of the piezo-spectroscopic techniques is that the average uniaxial piezo-spectroscopic coefficients (PS), P_{uni}, characterizing the linear dependence of the peak shift on stress, strongly depends on many material parameters, and in particular in processing derived parameters such as grain size, presence of other phases, porosity, etc. Hence, a preliminary calibration procedure is required in every case for determining the P_{uni} value specific to each material.

3. Experimental procedures

3.1. Material preparation

Starting powders of α-Al_2O_3 (Condea HPA 0.5, USA), with mean particle size of 0.35 μm and specific surface area of 9.5 m^2/g, and ZrO_2 stabilised with 3 mol% Y_2O_3, YTZP, (TZ3YS, TOSOH, Japan), with a mean particle size of 0.4 μm and a specific surface area of 6.7 m^2/g, were employed. A polyelectrolyte (Dolapix CE 64, Zschimmer & Schwarz, Germany) was used for powder dispersion in deionised water as dispersing media. A water-based polymeric emulsion Mowilith DM 765 E (Celanese, Spain), with a Tg of –6°C and solid content 50 vol%, particle size 0.05–0.15 μm was used as binder emulsion.

The processing route established previously [7, 8], which involves the tape casting of individual tapes with different compositions and further stacking them to form monolithic composites and symmetrical laminates was used in the present work. Water-based tape cast tapes having compositions of 95 vol% α-Al_2O_3—5 vol% YTZP (named A-5YTZP, slurry with 47 vol% solids content) and 60 vol% α-Al_2O_3—40 vol% YTZP (named A-40YTZP, slurry with 50 vol% solids content) were prepared. The stabilisation of the slurries with the dispersant (dispersant with 0.8 and 0.7 wt% solids for A-5YTZP and A-40YTZP, respectively) was performed by ball milling using alumina balls for 4 h. 5 wt% binder, referred to solids content, was added to the deflocculated suspensions and they were mixed using a blade mixer for 30 min. The tape casting was performed on stationary polypropylene film using a moving tape casting device with two doctor blades (laboratory developed device [7]). The final casting parameters were 10 mm/s of casting velocity and 500 μm of gap height between the blades and the carrier film. After drying in air for 24 h the green ceramic tapes were subjected to further drying at 60°C degrees for 48 h. The final thickness of the green tapes obtained varied between 480–520 μm. Round shaped tapes were used to avoid heterogeneous stress distribution within the specimens during pressing [7], for this purpose the final shaping by punching out round shape (Ø 60 mm) pieces of tape was performed. Seven tapes were stacked consequentially to form the symmetrical laminate and composite pieces as shown in Fig. 1a, applying the gluing agent at the interfaces. The pieces were cold uniaxially pressed under 18 MPa of pressure. Full details of tape pre-treatment, gluing agent application and the pressing procedure are given elsewhere [7, 8].

Two discs of each composition were left in their as pressed shape (diameter Ø 60 mm) and the others were cut into bars (approximately 30 × 7 × 4.1 mm) for sintering. Prior to sintering the surfaces of the green pieces were smoothened using sandpaper. Binder burn out and sintering were performed in a single thermal treatment

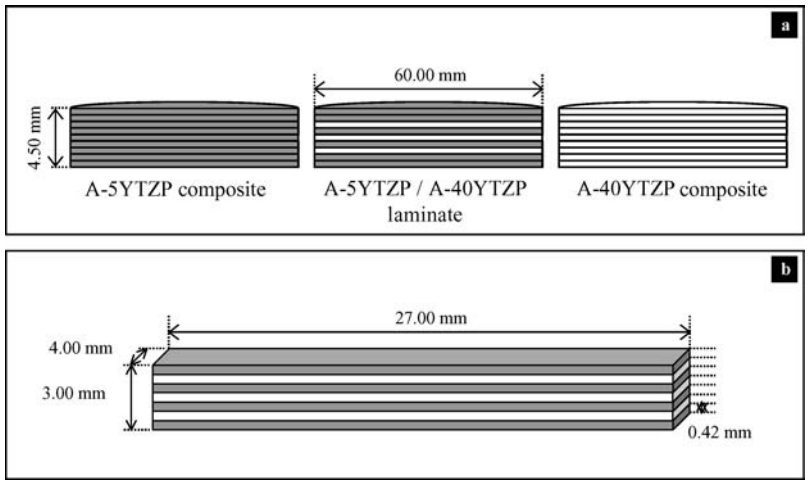

Figure 1 Preparation of laminated structures by piling up individual green ceramic tapes. (a) Cross section of stacked symmetrical laminate and monolithic composite pieces. (b) Final geometry of symmetrical laminate sample fabricated.

cycle. The binder burn out was carried out at a heating rate of 1°C/min up to 600°C, with a dwell time of 30 min. Sintering was carried out by increasing the temperature (heating rate of 2°C/min) up to 1550°C with a dwell time of 2 h. Sintered composite and laminate bars were grinded to obtain the samples with the final geometry (Fig. 1b). The longitudinal face (perpendicular to the constituent tapes) used for residual stress assessment was polished successively using 9, 6 and 1 μm diamond paste and its edges were rounded during the polishing operation.

3.2. Characterization of obtained composites

Sintered density was determined using Archimedes method in distilled water. Relative sintered densities were calculated as % of the calculated theoretical density for each composition, using 3.99 gr/cm^3 for α–Al_2O_3 (ASTM 42–1468) and 6.10 gr/cm^3 for YTZP (ASTM 83–113). The Young's modulus (E) and the shear modulus of the composites were determined from the resonance frequency of the as sintered discs tested by impact in flexural and torsional modes (GrindoSonic MK5, J.W. Lemmens-Electronica N.V., Belgium). The average coefficient of thermal expansion (α) between 1200°C and room temperature was calculated from the thermal expansion curves recorded using bars (10 × 4 × 3 mm) in a dilatometer with alumina support (Setaram, Setsys-16/18, France) and corrected for alumina expansion.

Three samples were used for determination of density, Young's modulus and average thermal expansion coefficient of each composite; reported values are the average of the obtained data and errors are the standard deviation.

3.3. Residual stress assessment

The level and sign of the expected residual stresses was evaluated using the simplified model of a symmetric plate constituted by alternate layers of the same thickness having a uniform biaxial distribution of stresses across each layer [1]. In this case, the stresses developed in a laminate made by two kinds of layers, a and b, are given by:

$$\sigma_a = -\frac{\Delta\varepsilon \mathrm{E}'_a}{1 + \frac{E'_a n_a t_a}{E'_b n_b t_b}} \tag{2}$$

$$\sigma_b = -\sigma_a \frac{n_a}{n_b}\frac{t_a}{t_b} \tag{3}$$

where $\Delta\varepsilon$ is the thermal expansion mismatch between the layers:

$$\Delta\varepsilon = \int_{20}^{1200} (\alpha_b - \alpha_a) dT \tag{4}$$

and $n_{a,b}$, $t_{a,b}$ and $\alpha_{a,b}$ are the number of layers, the thickness and the CTE of each composition, and $\mathrm{E}'_{a,b}$ is the reduced Young's modulus:

$$E'_i = \frac{E_i}{1 - \nu_i} \tag{5}$$

In the system examined (Fig. 1), a and b correspond to the A-5YTZP and A-40 YTZP layers, respectively, and $t_a = t_b = 420$ μm.

To collect fluorescence spectra, the spectrometer apparatus (ISA, T 64000 Jovin-Yvon), as excitation source, an argon-ion laser operating at a wavelength of 488 nm with a power of 400 mW. For obtaining micron-scale magnification, an optical microscope lens was used both to focus the laser on the sample and to collect the scattered signal. Scattered frequencies were analyzed on a triple monochromator equipped with a charge coupled device (CCD) camera. When focussed by an optical microscope, the dimension of the laser spot on the samples was 5 mm (i.e., using a ×20 optical lens). Thermal and instrumental fluctuations were compensated by monitoring the spectrum from a Hg/Ne discharge lamp. The recorded spectra were analysed using commercial software (LabSpec 4.02,

TABLE I Salient piezo-spectroscopic characteristics of the investigated composites

Peak	Π_{uni} (cm^{-1}/GPa)	Π_{hydro} (cm^{-1}/GPa)	R^2	Unstressed peak position (cm^{-1})
A-5YTZP				
R1	2.79 ± 0.01	8.36 ± 0.03	0.998	14406.96 ± 0.01
R2	2.94 ± 0.01	8.82 ± 0.03	0.999	14404.87 ± 0.01
A-40YTZP				
R1	2.63 ± 0.01	7.89 ± 0.03	0.997	14436.92 ± 0.01
R2	2.67 ± 0.01	8.01 ± 0.03	0.999	14434.81 ± 0.01

Horiba/Jobin-Ivon). The frequency shifts were obtained by subtracting from the centre of the peak recorded under stress the centre frequency of the peak in the unstressed state.

Microscopic stress distributions were measured by collecting linear profiles of spectra on the specimen cross-sections. The automatically collected profiles of spectra were 10 mm-spaced. Specimens were placed on a mapping device (lateral resolution of 0.1 mm), which was connected to a personal computer to drive highly precise displacements (along both *X* and *Y* axes) on the specimen surface. Unstressed peak positions were obtained acquiring an array of 100 spectra on the surface of unstressed reference bars and averaging the values of the peak centre.

For the evaluation of PS coefficient the peak shift was recorded as a function of known stresses. To do so, bending bars of both composites were mounted on a four-point bending jig and loaded with a known load below fracture stress; after the load was applied, the whole jig was moved under the laser and spectra recorded every 40 mm from the compressive towards the tensile side of the specimen. To reduce the scattering of data hence improve PS coefficient determination, the calibration was repeated 5 times and the values obtained were averaged. The load was then converted to stress, *s*, using the standard four-point-bending elastic equation and the peak shift, Dn, plotted as a function of the applied stress. The average P_{uni} was obtained from the slope of the *s* versus Dn plot. Table I summarizes the values of salient piezo-spectroscopic characteristics of the ceramic polycrystals studied in the present investigation.

Whereas sapphire has a different coefficient P_{ii} for each cristallographic axis [9], the Al_2O_3 present in the composites is supposed to be polycrystalline and lacking any significant texture, so that the uniaxial coefficient is one of the three identical elements of the diagonal of piezo-spectroscopic tensor P_{ii}. To calculate the mean hydrostatic stress, the following assumption was made:

$$\sigma = \frac{\Delta\mu}{\Pi_{hydro}} = \frac{\Delta\mu}{3\Pi_{uni}}$$

where Dn is the shift of pea.

For stress measurement R1 band was used to avoid errors in fitting due to the superposition of a line of reference Hg/Ne lamp spectrum with R2 band. In relation to the weak deviation from linearity of R1 calibration line evidenced by He *et al*. [12], considering the high correlation coefficient obtained by lines referred to laminated material and the low stress measured, it was supposed to be negligible.

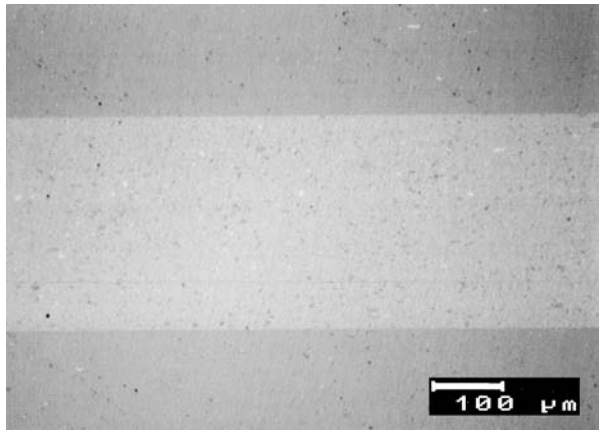

Figure 2 Photo of the cross section segment for A-5YTZP/A-40YTZP laminated structure. Darker layers A-5YTZP.

4. Results and discussion

Using the processing route described above, dense (≅99% of the theoretical), homogeneous monolithic and multilayered composites within the A-5YTZP/A-40YTZP system were obtained. The multilayered material presented straight and well defined interfaces between the constituent tapes, as shown in Fig. 2.

The properties of the compositions involved in the development of residual stresses within the laminate structure during cooling are summarized in Table II. Using Equations 2–5, maximum residual compressive stresses of about 160 MPa in the A-5YTZP layers and tensile stresses of about 220 MPa in the A-40YTZP layers are predicted.

Fig. 3 shows the macroscopic residual stress profile measured along the samples cross section. As mentioned, each profile is the average of five profiles collected along the cross section in order to reduce the scattering of data and to verify the uniformity of the residual stress field. The error relative to stress calculation is ±3%.

Two different geometries were analyzed: (i) a symmetric laminate composed of 7 alternate layers of A-5YTZP/A-40YTZP. As expected, A-5YTZP layers

TABLE II Properties of the investigated compositions involved in the development of residual stresses

Composite composition	$\rho_{sintered}$ (gr/cm^3)	$\rho_{sintered}$ (th.%)	Young's modulus (GPa)	Shear modulus (GPa)	Poisson coefficient	CTE α $_{(20–1200^\circ C)}$ ($\times 10^{-6}$/K)
A-5YTZP	4.03 ± 0.02	98.7 ± 0.1	389 ± 4	155 ± 2	0.25 ± 1	8.5
A-40YTZP	4.79 ± 0.01	99.2 ± 0.1	309 ± 2	121 ± 2	0.26 ± 1	9.2

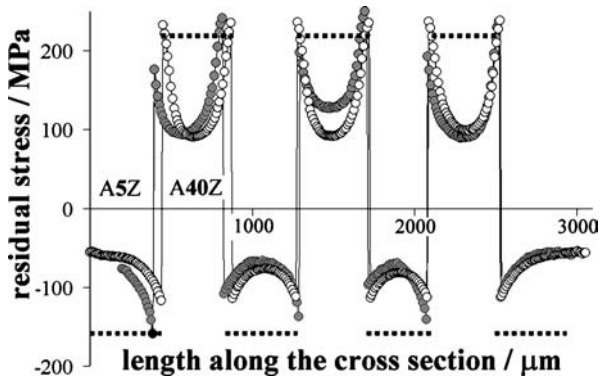

Figure 3 Profiles of macroscopic residual stress along the profile. The white dots refer to the symmetric sample, the grey dots to the asymmetric one. The error bands for residual stress value (±3%) are as large as the diameter of the dots. The labels A5Z and A40Z over each layer refer respectively to the composite A-5YTZP and A-40YTZP. Dotted lines indicated the theoretical streeses calculated for a biaxial system.

underwent compression, whereas A-40YTZP layers tension. Within the layers the stress was not constant but varied with a parabolic trend: the highest values were measured at interfaces, and a release moving toward the centre of the layer was observed. The values near the interface are close to the maximum values estimated by previous prediction. Moreover, a greater reduction could be seen in the A-40YTZP layer (from 230 to 100 MPa), compared to that seen in A-5YTZP layers (from −110 to –75 MPa): this difference is probably due to the different elastic modulus of the two composites (A-5YTZP being stiffer than A-40YTZP, Table II). (ii) The second geometry analyzed was similar to the previous one (4 A-5YTZP and 3 A-40YTZP alternated layers), but with one of the superficial A-5YTZP layers thinner than the other. The asymmetry affected the residual stress distribution especially in the thinner A-5YTZP external layer, where compressive stresses were higher than in the symmetric sample. The rest of the layers appeared to be influenced to a lesser degree, the stresses at the interfaces being systematically lower toward the direction of the thinner layer.

5. Conclusions

Ceramic multilayered Al_2O_3/YTZP composites were fabricated by water-based tape casting. The difference in thermal expansion coefficients induced a residual stress field whose magnitude and distribution were assessed by piezo-spectroscopy. Layers richer in Al_2O_3, for which the CTE is lower, were found to be under compressive stress, whereas layers with 40 vol% of YTZP underwent tensile stresses. Moreover, within the layers stress varied with a parabolic trend, the highest values being at the interfaces between the layers. The influence of geometric asymmetry on the magnitude and the distribution of residual stresses within multilayered laminate structures was also assessed. The lack of symmetry had a minor effect on the stress field, expressed in a form of asymmetric parabolic distribution of stresses measured.

Acknowledgments

This work was supported in part by the European Community's Human Potential Programme under contract HPRN-CT-2002-00203, [SICMAC]. Jonas Gurauskis acknowledges the financial support provided through this Programme. G. de Portu is also grateful to the Japan Society for the Promotion of Science (JSPS) and the Italian National Research Council (CNR) for the financial support of his work in Japan. The contribution of the Italian Ministry for Foreign Affair (MAE) which supported the creation of RIN is also gratefully acknowledged. This work was supported in part by CICYT MAT 2003-00836 and CAM, GRMAT0707–2004 (Spain).

References

1. T. CHARTIER, D. MERLE and J. L. BESSON, *J. Eur. Ceram. Soc.* **15** (1) (1995) 101.
2. C. HILLMAN, Z. SUO and F. F. LANGE, *J. Am. Ceram. Soc.* **79** (8) (1996) 2127.
3. G. DE PORTU, L. MICELE and G. PEZZOTTI, *J. Mater. Sci. Lett* (2004) in press.
4. E. LUCCHINI and O. SBAIZERO, *J. Eur. Ceram. Soc.* **15** (1995) 975.
5. G. DE PORTU, L. MICELE and G. PEZZOTTI, *Appl. Spectr.* (2004) in press.
6. K. P. PLUCKNETT, C. H. CÁCERES, C. HUGHES and D. WILKINSON, *J. Am. Ceram. Soc.* **77** (8) (1994) 2145.
7. J. GURAUSKIS, A. J. SÁNCHEZ-HERENCIA and C. BAUDÍN, *J. Eur. Ceram. Soc.* (2004) in press, *Corrected Proof.*
8. J. GURAUSKIS, A. J. SÁNCHEZ-HERENCIA and C. BAUDÍN, *ibid.* (2004) in press.
9. L. GRABNER, *J. App. Phys.* **49** (1978) 580.
10. V. SERGO, D. M. LIPKIN, G. DE PORTU and D. R. CLARKE, *J. Am. Ceram. Soc.* **80** (7) (1997) 1633.
11. G. DE PORTU, L. MICELE, Y. SEKIGUCHI and G. PEZZOTTI, *Acta Materialia* (2004) in press.
12. J. HE and D. R. CLARKE, *J. Am. Ceram. Soc.* **78** (5) (1995) 1347.

Received 3 February
and accepted 26 May 2005